The *lss* Supernodulation Mutant of *Medicago truncatula* Reduces Expression of the *SUNN* Gene[1][OA]

Elise Schnabel[2], Arijit Mukherjee[2,3], Lucinda Smith, Tessema Kassaw, Sharon Long, and Julia Frugoli*

Department of Genetics and Biochemistry, Clemson University, Clemson, South Carolina 29634 (E.S., A.M., T.K., J.F.); and Department of Biology, Stanford University, Palo Alto, California 94035 (L.S., S.L.)

The number of nodules that form in a legume when interacting with compatible rhizobia is regulated by the plant. We report the identification of a mutant in nodule regulation in *Medicago truncatula, like sunn supernodulator* (*lss*), which displays shoot-controlled supernodulation and short roots, similar to *sunn* mutants. In contrast with the *sunn-1* mutant, nodulation in the *lss* mutant is more extensive and is less sensitive to nitrate and ethylene, resembling the *sunn-4* presumed null allele phenotype. Although the *lss* locus maps to the *SUNN* region of linkage group 4 and *sunn* and *lss* do not complement each other, there is no mutation in the genomic copy of the *SUNN* gene or in the 15-kb surrounding region in the *lss* mutant. However, expression of the *SUNN* gene in the shoots of *lss* plants is greatly reduced compared with wild-type plants. Analysis of cDNA from plants heterozygous for *lss* indicates that *lss* is a cis-acting factor affecting the expression of *SUNN*, and documented reversion events show it to be unstable, suggesting a possible reversible DNA rearrangement or an epigenetic change in the *lss* mutant. Assessment of the *SUNN* promoter revealed low levels of cytosine methylation in the 700-bp region proximal to the predicted transcription start site in both wild-type and *lss* plants, indicating that promoter hypermethylation is not responsible for the suppression of *SUNN* expression in *lss*. Thus, *lss* represents either a distal novel locus within the mapped region affecting *SUNN* expression or an uncharacterized epigenetic modification at the *SUNN* locus.

Symbiosis between two organisms requires cross-species communication, often using molecular signals. For a symbiosis to be evolutionarily successful, there must be a balance of costs and benefits between the two organisms; the tradeoffs made by each to establish the association must be balanced by benefits gained. The interaction of legumes and nitrogen-fixing rhizobia has several such tradeoffs. The plant alters its developmental program to provide a home for the bacteria in specialized structures called nodules. In exchange for this energy-intensive development, the plant receives nitrogen in a biologically usable form from the bacteria. The bacteria also change their developmental program, differentiating into bacteroids, and receive energy and carbon skeletons from the plant in exchange for the nitrogen they provide. The application of molecular genetic techniques to the study of this interaction has yielded many new insights. Because the biological cost to the plant of nodule formation and function is estimated at 12 to 17 g of carbon per gram of nitrogen (Crawford et al., 2000), the host plant tightly regulates the number and positions of the nodules that form. Plants that have lost this regulation through mutation form excessive nodules, resulting in a phenotype termed hypernodulation or supernodulation.

At the molecular level, flavonoids secreted into the soil by the plant induce the expression of rhizobial *nod* genes, resulting in the synthesis of a modified (substituted) lipochitin oligosaccharide called the Nod factor. A species-specific interaction between the Nod factor and the molecular receptor(s) on the plant root hairs causes a set of physical and genetic changes that allow the bacteria to enter the plant tissue. The root hair grows so as to curl around and entrap the bacteria, forming a structure termed a crozier, or shepherd's crook. In legumes that maintain persistent nodule meristems, such as alfalfa (*Medicago sativa*) and pea (*Pisum sativum*), the plant cells display cytoskeletal rearrangements that accompany cell division and that facilitate the growth of a plant-generated infection thread from the root hair cell to the inner cortical cells. At the same time, genetic reprogramming of the inner cortical cells adjacent to the xylem poles results in the formation of a nodule meristem that will eventually receive the bacteria in intracellular compartments called symbiosomes. Once inside the nodule in symbiosomes, the rhizobia will express the nitrogenase

enzyme and fix nitrogen for the plant, while obtaining carbon skeletons across the symbiosome membrane from the plant in return. This symbiosis allows legumes to grow in the absence of available soil nitrogen. The plant regulates this process: in the presence of available soil nitrogen, nodulation is suppressed (for review, see Riely et al., 2006; Stacey et al., 2006; Oldroyd and Downie, 2008).

Both physiology and genetics have been used to explore the mechanism of nodule number control. In the case of *Medicago truncatula*, the plant limits the number of infection threads that proceed all the way to the inner cortex and the number of nodule meristems that initiate (Penmetsa and Cook, 1997). Consequently, while numerous infection threads may initiate, wild-type seedlings form only seven to 10 nodules when grown under aeroponic conditions (Penmetsa and Cook, 1997). The plant exerts several further levels of control on nodule development. Nodulation occurs only in the expansion zone of the root, and nodules form predominantly adjacent to xylem poles. Split-root and grafting experiments have demonstrated that in many legumes, control of nodule number involves long-distance signaling from the shoot to the root (Bauer, 1981; Kosslak and Bohlool, 1984; Caetano-Anollés and Gresshoff, 1991; Sagan and Duc, 1996; Krusell et al., 2002; Nishimura et al., 2002a; Penmetsa et al., 2003; Oka-Kira and Kawaguchi, 2006). Other evidence shows that local tissues also have a role in signaling: (1) in some mutants, the root genotype controls nodule number; and (2) application of hormones directly to the roots can change nodule number (Jacobsen and Feenstra, 1984; Hirsch and Fang, 1994; Prayitno et al., 2006; Ishikawa et al., 2008). Analysis of local and long-range auxin transport in nodulating legumes showed that inoculation is accompanied by a local change in auxin transport that is thought to be necessary for nodule initiation (Mathesius et al., 1998; Boot et al., 1999; Pacios Bras et al., 2003; Huo et al., 2006; Subramanian et al., 2006, 2007; Zhang et al., 2007a) and by a decrease in long-range auxin flux from the shoot to the root. Both changes appear to be coordinated with the autoregulation of nodulation (van Noorden et al., 2006).

At present, *sunn* and *skl* are the only published supernodulation mutants in *M. truncatula*. Each is represented by multiple alleles. *SUNN* encodes a Leu-rich repeat receptor kinase with homology to Arabidopsis (*Arabidopsis thaliana*) *CLAVATA1* (*CLV1*), although it shows none of the meristem defects of Arabidopsis *clv* mutants (Schnabel et al., 2005). Orthologs with very similar phenotypes have been isolated from soybean (*Glycine max*), *Lotus japonicus*, and pea (Krusell et al., 2002; Nishimura et al., 2002a; Searle et al., 2003). Plants with a mutated *SUNN* gene have shorter roots and 5- to 10-fold more nodules when compared with wild-type plants (Penmetsa et al., 2003; Schnabel et al., 2005; van Noorden et al., 2006). Several mutations in the *SUNN* gene have been identified: the mutation in the *sunn-1* allele results in an amino acid

change in the kinase domain of the protein, *sunn-2* is an amino acid change in the Leu-rich repeat region, while the mutation in the *sunn-4* allele results in a truncation of the message immediately after the initial signal peptide sequence and is presumed to act as a null mutation with no *SUNN* protein produced (Schnabel et al., 2005).

The *SKL* gene encodes a protein with homology to Arabidopsis EIN2 (a component of the ethylene signaling pathway), and the mutants have several ethylene-related phenotypes such as long roots in addition to nodulation defects (Penmetsa et al., 2008): excessive nodule number and loss of spatial control (position relative to xylem) of nodule formation (Penmetsa and Cook, 1997). An ortholog to *SKL* affecting nodulation in other legumes has yet to be identified, but overexpression in *L. japonicus* of a dominant negative allele of another Arabidopsis ethylene response gene, *ETR1*, increases nodule number (Gresshoff et al., 2009).

Supernodulation mutants with no clear ortholog yet in *M. truncatula* have been identified in other legumes. The *astray* mutant in *L. japonicus* results in moderately increased nodulation (2-fold versus the 5- to 10-fold usually associated with hypernodulation). The corresponding gene encodes a basic Leu zipper protein with a ring finger motif similar to Arabidopsis HY5 (Nishimura et al., 2002b). Another *L. japonicus* supernodulation mutant, *klavier*, causes pleiotropic effects on flowering time, plant stature, and venation (Oka-Kira et al., 2005). The *rdh1* and *tml* mutants of *L. japonicus* also display a supernodulation phenotype; grafting experiments have shown that the signal controlling nodule number in these mutants is root derived (Ishikawa et al., 2008; Magori et al., 2009). Mutants described only at the phenotype level include the *Phaseolus vulgaris ntsn* supernodulation mutant (Park and Buttery, 1989) and two pea mutants, *sym28*, a shoot-controlled nodulator with a fasciation phenotype (Sagan and Duc, 1996), and *nod3*, a root-controlled supernodulation mutant (Jacobsen and Feenstra, 1984).

Here, we report a novel *M. truncatula* supernodulation mutant distinct from *skl* and the *Pisum* and *Lotus* mutants described above. The *like sunn supernodulator* (*lss*) mutation interacts genetically with *sunn*, yet it is not a lesion in the *SUNN* gene proper or in the adjacent regulatory sequences. Nodulation in *lss* is more extensive than in *sunn-1* and is less sensitive to nitrate and ethylene. The expression of the *SUNN* gene is greatly reduced in *lss* mutants, and overall, the *lss* phenotype resembles the phenotype of the *sunn-4* presumed null mutation. Results of our analyses are consistent with *lss* exerting an epigenetic effect on *SUNN* expression.

RESULTS

The *lss* Mutation Is Recessive, with Supernodulation and Short-Root Phenotypes Resembling Those of the *sunn* Mutation

Based on a visual screen for altered nodule number, we identified a spontaneously occurring supernodu-

lation mutant from the Jemalong cultivar (from which the wild-type A17 line was derived), which we designated *lss*. Following inoculation with rhizobia under nitrogen-limiting conditions, plants carrying the mutation have a 10- to 15-fold increase in nodule number and shorter roots than wild-type plants. When grown in aeroponic conditions side by side with the wild type and *sunn-1* and *sunn-4* mutants, plants bearing the *lss* mutation strongly resemble the previously identified *sunn-4* mutant (assay done at 10 d post inoculation; Fig. 1; Penmetsa et al., 2003; Schnabel et al., 2005). Both *lss* and *sunn-4* form significantly more nodules than *sunn-1*.

Consistent with previous work, we observed little to no nodulation on wild-type plants supplied with 10 mM nitrate as either NH_4NO_3 or KNO_3 (Fig. 1A). In contrast, *lss* mutant plants demonstrate nitrate-tolerant nodulation. When grown aeroponically in the presence of 10 mM ammonium nitrate and compared with *sunn-1* and *sunn-4* mutant plants, *lss* mutant plants form more nodules than wild-type or *sunn-1* plants and have nodule numbers similar to *sunn-4* plants (Fig. 1A).

We measured the root length of nodulated and uninoculated plants. In nitrate-free conditions, nodulated *sunn-1*, *sunn-4*, and *lss* roots grew to only about half the length of wild-type roots (Fig. 1B, black bars). In the presence of 10 mM NH_4NO_3, all genotypes, including the wild type, displayed the same short-root phenotype when nodulated (Fig. 1B, striped bars). Since supernodulator roots grew the same under both nitrate conditions, we wondered if their short-root phenotype was due to excessive nodule development and could not be further reduced by nitrate. However, when plants were grown under nonnodulating conditions (no rhizobia) and in nonlimiting nitrate, *sunn-1* and *lss* still exhibited the short-root phenotype (Fig. 2; $P < 0.001$, Student's t test).

Grafting experiments revealed that for *lss* mutants, the genotype of the shoot tissue determines the number of nodules that form (Table I), as was previously shown for the *SUNN* gene (Penmetsa et al., 2003).

Because of the similar nodulation, root length, and shoot-control phenotypes, we named the mutant *lss*.

To define the map position of the *lss* locus, pollen from the wild-type polymorphic mapping ecotype A20 was used in crosses with homozygous *lss* individuals. All four F1 heterozygotes derived from this cross displayed wild-type nodulation and root length. In a backcross of *lss* to parental A17, all eight progeny also displayed wild-type nodule number and root length. Both lines of evidence indicate that *lss* is a recessive allele. F2 progeny of the A20 cross ($n = 209$) were scored for nodule number 10 d post rhizobial inoculation; 44 plants displayed the supernodulation phenotype, while the remaining 165 individuals showed wild-type nodulation. The phenotypic ratio of 165:44 closely approximates 3:1 ($\chi^2 = 1.73$, $P < 0.05$) and is consistent with the phenotype resulting from a single gene mutation.

lss and *sunn-1* Mutants Have Different Responses to Ethylene

Because altered ethylene responses have been documented in previously published *M. truncatula* supernodulation mutants (Penmetsa and Cook, 1997; Oldroyd et al., 2001; Penmetsa et al., 2008), we tested the response of *lss* to ethylene. Previously, we had reported that nodulation in both *sunn-1* and wild-type A17 was reduced in the presence of 1-aminocyclopropane-1-carboxylic acid (ACC), an ethylene precursor (Penmetsa et al., 2003). We observed here that *lss*, *sunn-4*, and wild-type plants appeared less sensitive to ACC inhibition of nodulation than did *sunn-1* (Fig. 3A). Our standard growth conditions on plates include 0.1 μM aminoethoxyvinylglycine (AVG) added to the medium to inhibit excess ethylene biosynthesis and buildup on the plate, thus allowing plants to nodulate. Therefore, we tested nodulation on plates with a range of ACC and AVG concentrations that allowed high to low ethylene accumulation. AVG (low ethylene) increased nodulation in all plants but was more effective on wild-type, *sunn-4*, and *lss* plants than on *sunn-1* plants,

Figure 1. Nodulation and root phenotypes of the *lss* mutant. A, Average nodule number of 14-d-old plants grown under aeroponic conditions in the presence or absence of 10 mM nitrate in the form of KNO_3 or NH_4NO_3 ($n = 17$ to 25 plants per genotype) at 10 d post inoculation (pi). B, Average root length (in mm) of the same plants as in A. Error bars for all graphs indicate SE. When compared with the wild type, $P < 0.05$ by Student's t test for all comparisons within a treatment in A and the no-nitrate comparison in B.
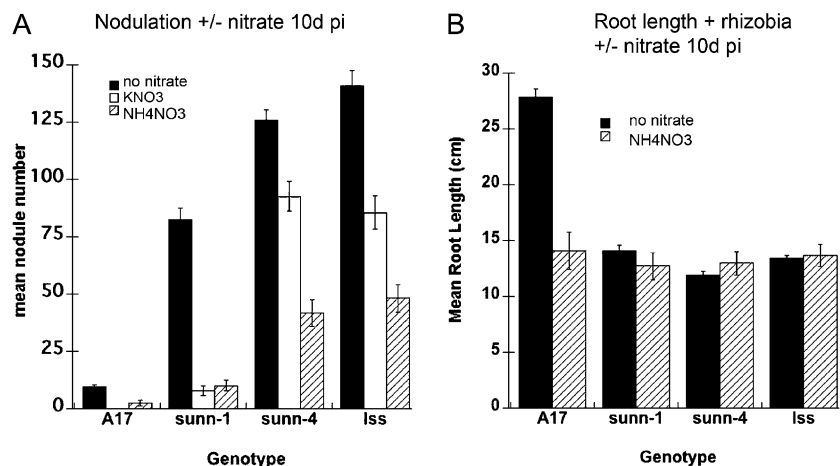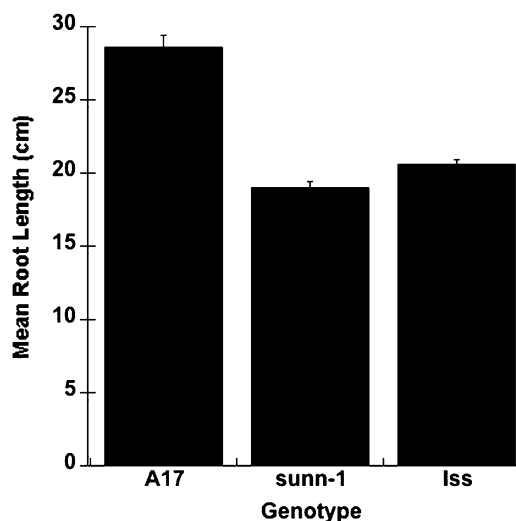
Figure 2. Root length of the *lss* mutant in the absence of rhizobia. Root length is shown for wild-type, *sunn-1*, and *lss* plants grown under aeroponic conditions in the presence of 5 mM NH_4NO_3 without rhizobia. This concentration of nitrate is not limiting for root growth. Data are from 14-d-old plants ($n = 24$–25 plants for *sunn-1* and A17 and $n = 40$ plants for *lss*). Error bars indicate SE. Both *sunn-1* and *lss* are significantly different from the wild type ($P < 0.001$ by Student's *t* test).

again indicating that *sunn-1* is more sensitive to ethylene (Fig. 3A). When suppression of nodulation was considered as a percentage of the normal nodulation observed under our standard conditions (0.1 μM AVG), relationships were more complex, but examining a subset of the data from Figure 3A in this manner revealed that the *sunn-1* nodulation response is more sensitive to ethylene than that of *sunn-4*, *lss*, or the wild type (Fig. 3B). Since this phenotypic distinction could involve differences in either ethylene perception or ethylene generation by the mutants, we measured ethylene production in the mutants versus the wild type after inoculation and compared it with the ethylene-insensitive *skl* supernodulator, which in our assay overproduced ethylene. Ethylene levels were the same in the wild type, both *sunn* alleles, and *lss*, suggesting that any observed difference in ethylene response is related to ethylene perception (Fig. 3C).

Genetic Interaction between *sunn* and *lss* Mutants

To test the allelism of *lss* with other published supernodulation mutants, we performed genetic crosses. A cross of *lss* and *skl1-1* (Penmetsa et al., 2008) resulted in five F1 plants showing wild-type nodulation and root length; this indicates that *lss* is not allelic to *skl*. To test the allelism of *lss* and *sunn*, we performed crosses to the *sunn-1*, *sunn-2*, and *sunn-4* mutants. As previously described, the *sunn-1* allele is a missense mutation in the kinase domain, *sunn-2* is a missense mutation in a residue between two Leu-rich repeats, and *sunn-4* is a truncated allele created by a nonsense mutation before the Leu-rich repeat region (Schnabel et al., 2005). The

phenotypic difference between the *sunn* mutants and *lss* in nodule number is quantitative and varies slightly between growth conditions; the F1 plants did not consistently show nodule number matching a single parental phenotype, but all F1 plants were supernodulators. The noncomplementation of *lss* and *sunn* alleles could be interpreted as evidence that *sunn* and *lss* are lesions in the same gene. Reciprocal crosses to *lss* were performed with the *sunn-1* allele. The phenotypes of the F1 generation of the reciprocal cross resembled those of the original cross, indicating that the noncomplementation was not due to parental imprinting.

The *lss* and *sunn* Mutations Map to the Same Region

A mapping cross of *lss* to the A20 ecotype yielded 3,662 F2 progeny, 692 of which displayed the *lss* phenotype. Using publicly available cleaved-amplified polymorphic sequence (CAPS) markers and some developed for this work (see "Materials and Methods"), we were able to identify recombination events in plants bearing the *lss* mutant phenotype that place the *lss* lesion on the lower arm of linkage group 4 near the marker DNABP on the *M. truncatula* linkage map (Fig. 4A). Markers between the ES10P20-2 and AJ16C13B CAPS markers displayed the homozygous A17 genotype on all *lss* homozygotes. Combined with data from the *M. truncatula* sequencing project, the recombination events allowed construction of a contig of sequenced bacterial artificial chromosomes (BACs) defining a segment of linkage group 4 of approximately 810 kb in length containing the *lss* mutation. Only the 61L2 BAC in the contig is not sequenced, but end sequences place it in a bridging position between 78C5 and 167K21. The *SUNN* gene is within this 810-kb region, as well as 174 other genes in this segment identified by the International Medicago Gene Annotation Group. Analysis of the International Medicago Gene Annotation Group annotation reveals that almost 20% of the sequence in this contig is annotated as retroelements and repetitive sequence elements. The recombination rate in the *lss* × A20 population is approximately half the rate in the *sunn-1* × A20 population, which we had previously identified as suppressed in recombination (Schnabel et al., 2003),

Table I. *Results of shoot/root grafting experiments with M. truncatula seedlings*

Genotypes are listed in columns 1 and 2, and nodulation was measured 11 to 17 d following mending of the graft and inoculation. Results are reported ±SD.

| Graft Shoot	Graft Root	Nodule No.	No. of Successful Grafts
Wild type	Wild type	18 ± 5	6
Wild type	*lss*	23 ± 7	12
lss	Wild type	75 ± 3	3
lss	*lss*	57 ± 13	8
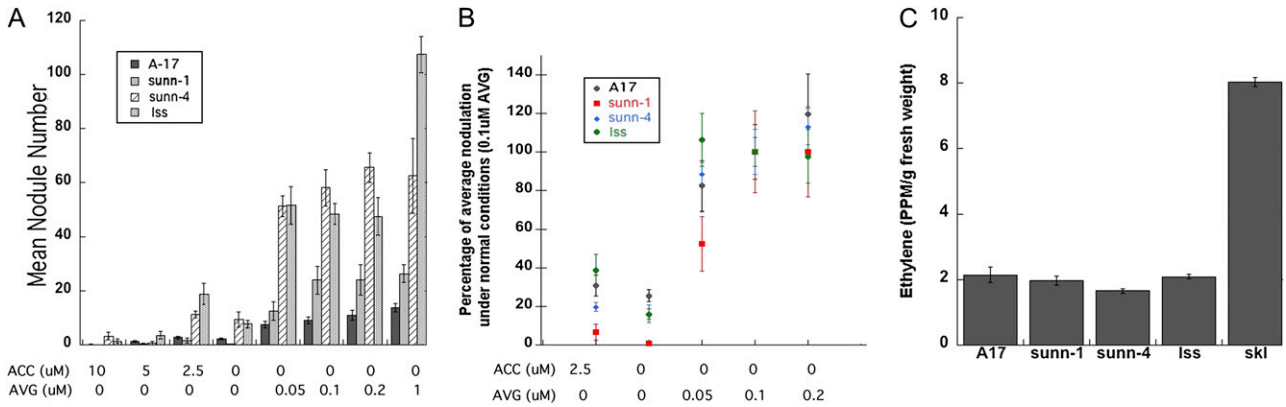
Figure 3. Ethylene-related phenotypes of the *lss* mutant. A, Average nodule number of A17 (wild-type), *sunn*, and *lss* plants grown on decreasing concentrations of the ethylene precursor ACC and increasing concentrations of the ethylene biosynthesis inhibitor AVG (*n* = 5–15 plants per genotype per treatment). Error bars indicate SE. B, A subset of the data in A displayed as a percentage of the normal nodule number seen under our standard conditions of 0.1 μM AVG. C, Ethylene content as parts per million per gram fresh weight of inoculated wild-type, *sunn-1*, *sunn-4*, and *lss* plants compared with the ethylene-insensitive *skl* mutant. Three plants of each genotype per sample were measured at 10 d post inoculation, with three biological replicates each. Error bars indicate SE.

and the suppressed region extends over a much larger region than observed in the original data mapping *SUNN*.

To confirm that *lss* was not a mutation in *SUNN*, in the linked gene *RLP1* (Schnabel et al., 2005), or in regulatory regions surrounding *SUNN*, we sequenced the *SUNN* region in *lss*. The sequenced DNA included the *SUNN* gene as well as the neighboring *RLP1* gene (Schnabel et al., 2005), the entire 6.4-kb region between *SUNN* and *RLP1*, and 7.2 kb past the *SUNN* 3′ untranslated region to the start of the next gene in *lss* plants. We found no DNA base changes in the se-
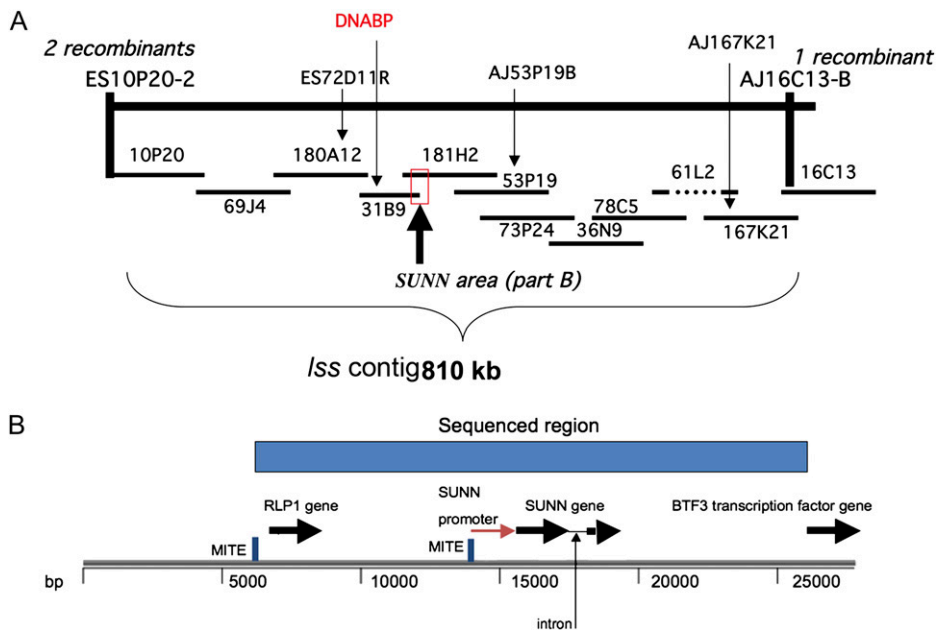
Figure 4. The region surrounding the *lss* lesion on linkage group 4. A, Contig containing the *lss* lesion with supporting BACs and location of recombination events from an F2 mapping population of A20 crossed to *lss*. DNABP (red) is a publicly available marker (http://www.medicago.org/genome/map_chr.php?chr=4). PCR markers shown above the chromosome line are based on sequence polymorphisms between A17 and A20 genotypes (see "Materials and Methods"). BAC numbers in the contig below the chromosome line refer to the Mt_ABb library. The 61L2 BAC is shown as a dashed line because it has only been end sequenced, so the length and sequence contents are uncertain. The region inside the red box is expanded in B. B, The region of the genome immediately surrounding the *SUNN* gene in A. Numbers refer to length in bases. Regions in blue have been completely sequenced and shown to be wild type in *lss* plants.

quenced regions from *lss* plants compared with wild-type plants (Fig. 4B).

The Expression of *SUNN* Is Altered in the *lss* Mutant

Since the phenotypes of *lss* and *sunn-1* mutant plants are most different from each other, we compared *SUNN* expression in *sunn-1* and *lss* plants. Previous work determined that the expression level of the *SUNN* gene in *sunn-1* plants was wild-type level in the shoots and reduced to about one-third of wild-type level in the roots (Schnabel et al., 2005). Analysis of *SUNN* expression levels in *lss* plants by real-time reverse transcription quantitative PCR (RT-qPCR) showed a similar reduction of *SUNN* message in *lss* roots (Fig. 5A) but an almost complete absence of *SUNN* expression in *lss* shoots (Fig. 5B). This unexpected result is discussed below. Plants heterozygous for the *lss* mutation, which have a wild-type nodulation phenotype, display an intermediate level of *SUNN* expression in the shoots (Fig. 5, C and D) and almost wild-type levels in the roots. In this second set of biological replicates, *SUNN* expression was undetectable in any tissue of the *lss* homozygote, but the zero value is within the range of error in Figure 5 (A and B).

Molecular Basis of Reduced *SUNN* Expression in *lss* Shoots

We reasoned that the lack of shoot expression of *SUNN* in *lss* plants could be due to a cis-element that

affects *SUNN* expression. If so, plants heterozygous for *lss* would have reduced *SUNN* expression, because the chromosome containing the *lss* lesion would not express the *SUNN* gene. To investigate this possibility, we created plants heterozygous for *lss* and the *sunn-2* mutation and for *lss* and the *sunn-1* mutation. In these plants, one copy of linkage group 4 carries a wild-type allele of *SUNN* and a mutant allele of *LSS*, while the other carries a mutant allele of *SUNN* (*sunn-2* or *sunn-1*, from which the messages can be distinguished from the wild type by restriction analysis of a PCR product from the cDNA) and a wild-type copy of *LSS* (Fig. 6A). This resulted in plants with the following genotypes: *SUNN lss/sunn-1 LSS* and *SUNN lss/sunn-2 LSS*. Analysis of cDNA generated from the shoots of these heterozygotes demonstrated that only the mutant *sunn-1* and *sunn-2* alleles (the ones on the same chromosome as wild-type *LSS*) were predominantly expressed in the heterozygote (Fig. 6B). Wild-type *SUNN* gene expression from the *SUNN lss* chromosome was very low to nonexistent, producing only a faint band (Fig. 6B, *sunn-1* gel) or no band (Fig. 6B, *sunn-2* gel).

Reversion Events

Over the course of the work described here, we noticed occasional revertants, progeny from *lss* parents that exhibited a wild-type root and nodulation phenotype. We wondered if these reversion events restored *SUNN* expression to normal levels. In two
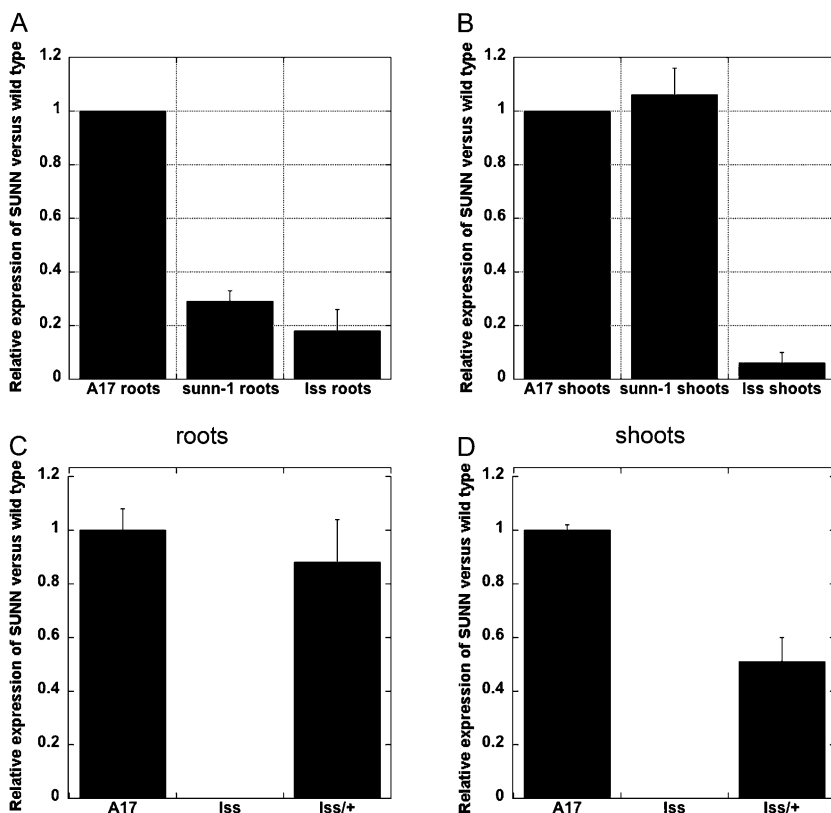
Figure 5. *SUNN* gene expression. A and B, Real-time RT-qPCR of relative *SUNN* expression levels in roots (A) and shoots (B) of wild-type, *sunn-1*, and *lss* plants. Error bars indicate SE of relative expression. Expression has been normalized to 1 in wild-type roots and shoots for comparison (see "Materials and Methods"). C and D, Real-time RT-qPCR of relative *SUNN* expression levels in roots (C) and shoots (D) of plants heterozygous for the *lss* mutation. The zero value for *SUNN* expression in *lss* in C and D is within the range of error in A and B. In all experiments, *SECRET AGENT* (Kuppusamy et al., 2004) was used as the RT-qPCR control.
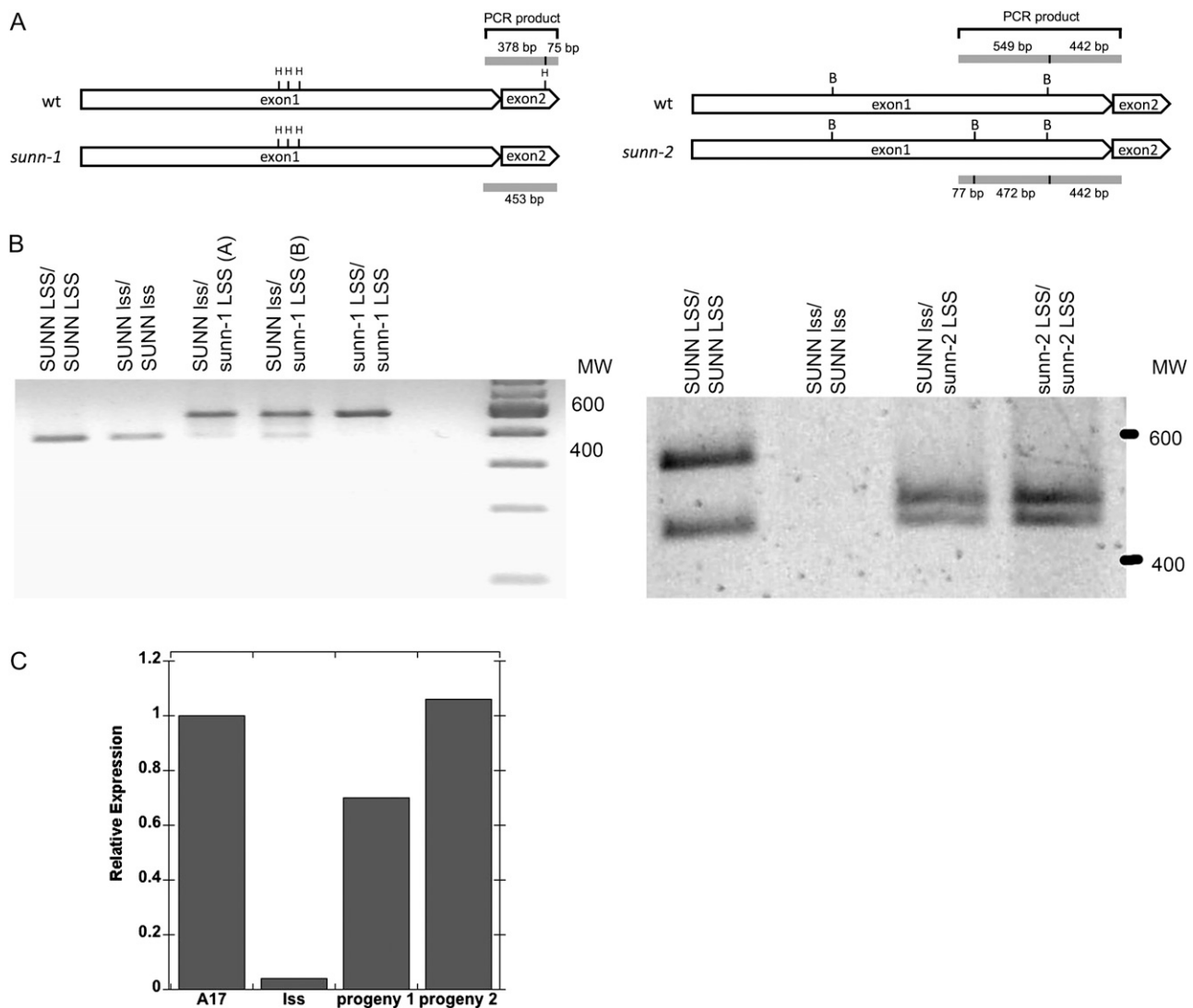
Figure 6. Origin of expressed *SUNN* in *sunn* LSS/*lss* SUNN plants. A, Diagram of mutation and PCR product locations and restriction sites used in B. H indicates a *Hae*III restriction site, while B indicates a *Bsm*AI site; within the PCR product, differential digestion is expected from the two alleles, giving bands of the sizes indicated in the diagram. wt, Wild type. B, Gel electrophoresis of PCR products generated by amplification of cDNA isolated from shoots of the indicated plants, with *SUNN*-specific primers, followed by digestion with the restriction enzyme *Hae*III or *Bsm*AI (see A and "Materials and Methods"). Digestion products from two heterozygotes (A and B) of *lss* and *sunn-1* are shown on the gel at left, and products from *lss* and *sunn-2* are shown at right. Note that in both cases, a band under 100 bases is also generated; these have been left off the image for simplicity, as the sizes of the major bands are diagnostic. MW, Molecular weight in bp. C, Real-time RT-qPCR of relative *SUNN* expression levels in shoots of A17, *lss*, and two F3 progeny of a *lss* revertant. The F2 parent plant segregated only wild-type plants, indicating that it was now homozygous for the reversion event.

separate experiments, three revertants were isolated from a total of 600 *lss* homozygotes grown from two independent batches of seed. The three revertants displayed a wild-type level of nodulation and had longer roots compared with the supernodulators. Selfing of the revertants and phenotypic analysis of their progeny produced segregation of a wild-type level of nodulation in a 3:1 ratio with supernodulators ($\chi^2 = 0.201$, $P < 0.05$), suggesting that one copy of the *lss* lesion was still present. We identified an F2 offspring of a revertant that segregated only wild-type plants in

the F3 generation. We used this small sample of plants presumably homozygous for the reversion event to ask if these reversion events restored *SUNN* expression to normal levels. Examination of the expression level of the *SUNN* gene in the shoots of two F3 individuals by RT-qPCR showed a return to normal levels of *SUNN* expression (Fig. 6C).

In a phenotypic analysis of F2 plants from the selfed F1 generation of the *sunn-1 lss* cross, 29 plants from a total of 308 individuals had wild-type nodulation. The remaining 279 plants displayed a supernodulation

phenotype. This result is unexpected if the two muta-
tions are in the same gene, but because of the apparent
close linkage of the two mutations, it is also highly
unlikely that these wild-type plants represent recom-
bination events between two linked genes. It remains
possible that these wild-type plants are reversions of
the *lss* phenotype.

Methylation Analysis

We wondered if changes in methylation of the
SUNN promoter could explain the origin of the low
expression of *SUNN* in *lss* plants, the observed rever-
sion events, and the wild-type progeny observed in
the F2 plants resulting from a cross between *sunn* and
lss plants. We analyzed the methylation status of the
SUNN promoter in young leaves of wild-type and *lss*
plants (the same tissue type used in Fig. 6) by bisulfite
genomic sequencing. Four overlapping fragments
selectively amplified from the lower strand of the
bisulfite-converted DNA of the 1.3-kb region upstream

of the start codon (−1,295 to −67) were used to
evaluate the overall methylation status of the *SUNN*
promoter. The resulting data represent approximately
half of the Cs in the *SUNN* promoter region and
include 11 CG, nine CHG, and 146 CHH sites, where H
may be A, T, or C (Fig. 7A).

The pattern of DNA methylation in this region did
not differ dramatically between the wild type and *lss*.
In the region −800 to −67, which includes the pre-
dicted transcription start site, little to no methylation
was detected. In contrast, within the predicted 184-
bp miniature inverted repeat transposable element
(MITE) located at positions −1,333 to −1,150, methyl-
ation was predominant, and methylation was common
in the flanking 300 to 400 bases in all contexts (CG,
CHG, CHH).

One small area downstream of the MITE displayed
minor differences in methylation between wild-type
and *lss* plants in our experiment (Fig. 7A, bracket). In
each case, within the region, methylation was slightly
lower in *lss* plants than in wild-type or revertant
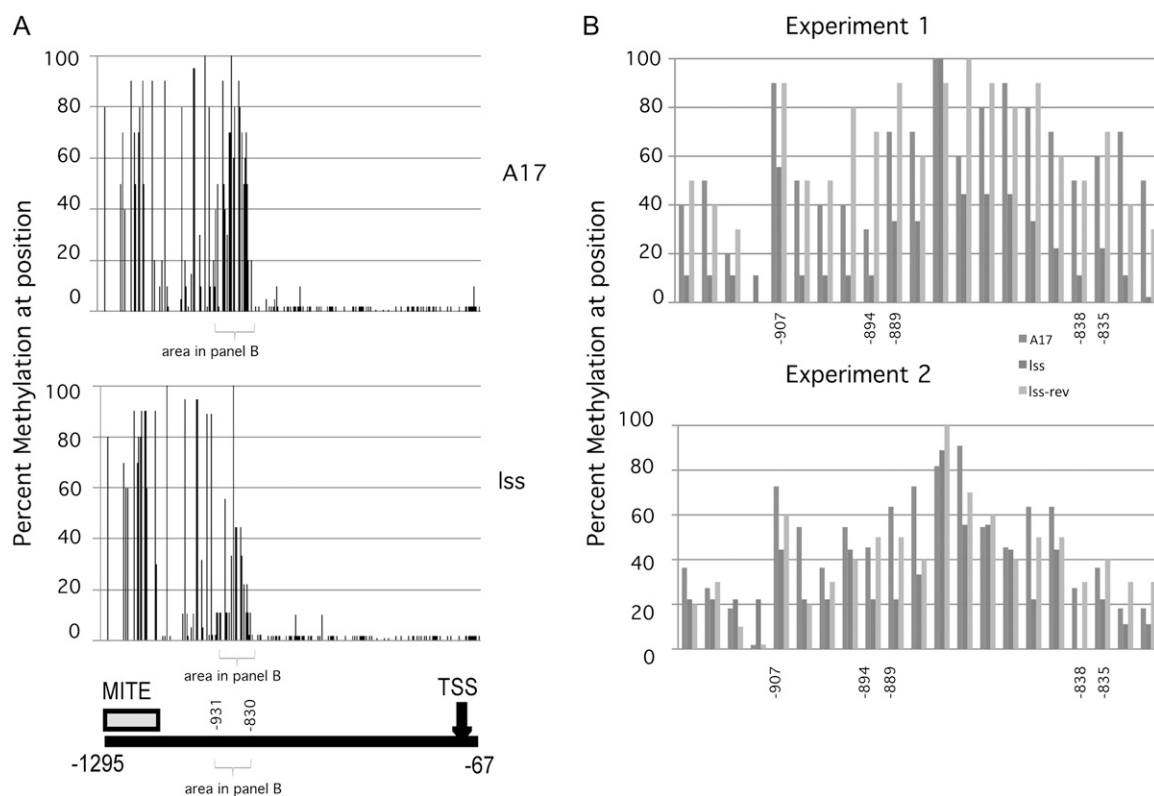
Figure 7. Methylation analysis of the *SUNN* promoter in wild-type and *lss* plants. A, Percentage of modified Cs in the *SUNN*
promoter in wild-type A17 (top) and *lss* mutant (bottom) plants in DNA from shoot tissue. Each tick mark across the x axis denotes
a C in the lower strand sequence. The y axis shows the percentage of time that C was methylated in the sequencing of 10 clones.
Some variation is expected due to the size of the sample. The bracket indicates an area of interest evaluated in B. The diagram
below shows the position of the MITE and the bracketed region relative to the x axis (see text). B, Results of bisulfite sequencing of
the area of interest from A in matched tissue from wild-type (A17; dark gray), *lss* (medium gray), and *lss* revertant (light gray)
plants in two independent experiments. The bases indicated by number are either the bases delineating the region (in A) or
instances in which a consistent pattern of small differences in methylation was seen (in B), but always biased toward greater
methylation in plants expressing *SUNN*. Base numbers refer to GenBank accession number AY769943.

Schnabel et al.

plants. To ascertain if these slight differences were contributing to the reduced *SUNN* expression we observed in *lss* plants, we followed up with bisulfite genomic sequencing from young leaves of a *lss* revertant and a second round of bisulfite genomic sequencing on DNA isolated from leaves of younger wild-type, *lss*, and *lss* revertant plants (Fig. 7B). Both experiments used types of tissue in which differential expression of *SUNN* between wild-type and *lss* plants had been confirmed. This allowed us to observe the variability present in our bisulfite sequencing assay as well as to compare the three plant lines. In most cases in which a small difference in methylation was detected, it was within the noise of the experiment and did not consistently occur between experiments. In five cases indicated by base numbers internal to the graph axis in Figure 7B, a base was more often methylated in wild-type and *lss* revertant plants than in *lss* plants by 10% to 30% in both experiments. Analysis of the SUNN promoter at the PLACE database (www.dna.affrc.go.jp/PLACE; Higo et al., 1999) did not identify these bases as part of any recognized promoter motif.

DISCUSSION

The *lss* mutation in *M. truncatula* is named for its similarity to the *sunn* mutation when the phenotypes of nodule number and root length are compared (Figs. 1 and 2) and because of the shoot control of the supernodulation phenotype (Table I). It also maps to the same region of the genome as the *sunn* mutation (Fig. 4) and does not rescue the *sunn* mutation when heterozygous. However, the *lss* mutant differs from *sunn-1* in nodulation regulation by nitrate (Fig. 1A), nodulation sensitivity to ethylene (Fig. 3), and gene expression phenotypes (Fig. 5); in these cases, *lss* behaves like the *sunn-4* presumed null allele. These data and the lack of any DNA lesions in the *SUNN* gene and the surrounding area in *lss* mutants imply that *lss* is a novel recessive mutation in *M. truncatula* that results in a supernodulation phenotype due to insufficient *SUNN* expression. The observation of putative reversion events suggests an epigenetic effect, but this effect is not through increased methylation of the promoter of the *SUNN* gene (Fig. 7).

With the exception of the *astray* mutant and the root-controlled *rdh1* and *skl* mutants discussed in the introduction, all published supernodulation mutants show at least partial nitrate-tolerant nodulation, including the *sunn* mutant (Jacobsen and Feenstra, 1984; Carroll et al., 1985a, 1985b; Park and Buttery, 1989; Sagan and Duc, 1996; Wopereis et al., 2000; Oka-Kira et al., 2005; Schnabel et al., 2005; Magori et al., 2009). However, we saw differential response to nitrate when comparing *lss*, *sunn-4*, and *sunn-1* nodulation on NH_4NO_3 or KNO_3 (Fig. 1B). The *sunn-4* and *lss* mutants continued to hypernodulate in the presence of nitrate, while *sunn-1* nodule number was significantly reduced in both KNO_3 and NH_4NO_3 compared with

no-nitrate conditions. This suggests that *sunn-1* mutants sense and respond to the presence of nitrate differently than *sunn-4* and *lss* plants, which continue to supernodulate in the presence of both KNO_3 and NH_4NO_3. Both *sunn-4* and *lss* presumably have little or no SUNN protein, implying that the sensing or response mechanism for nitrate regulation of nodulation requires SUNN.

Nitrate has been shown to inhibit nodulation by the induction of ethylene and by altering levels of flavonoids, auxins, and cytokinins (Coronado et al., 1995; Caba et al., 1998; Mathesius et al., 2000). Here, we found differences in ethylene response between the *sunn-1* allele and *lss*. The *sunn-4* and *lss* plants are more phenotypically similar to wild-type plants than *sunn-1* plants, being less sensitive to ethylene's effects on nodulation (Fig. 3, A and B), yet they all produce similar amounts of ethylene on a per gram fresh weight basis (Fig. 3C). Increasing ethylene by adding ACC or decreasing ethylene by adding AVG (Fig. 3, A and B) reveals a differential response between *sunn-1* compared with *lss*, *sunn-4*, and the wild type over a range of ethylene concentrations.

Because of the dramatic drop in *SUNN* expression in the shoots of *lss* plants (Fig. 5), we speculate that the phenotypic differences above result from insufficient *SUNN* expression in *lss* plants versus the expression of a mutant protein in *sunn-1* plants. The *sunn-4* mutant, which is presumed to lack SUNN protein, phenocopies *lss* in nitrate response (Fig. 1) and ethylene response (Fig. 3), suggesting that reduced *SUNN* expression causes the *lss* phenotype.

The lack of complementation in *sunn LSS/SUNN lss* plants can be explained by the reduced level of expression of the wild-type copy of the *SUNN* gene in *lss* heterozygotes (Fig. 4D) and is further supported by the observation that the *sunn-1* mutant has a hemizygous phenotype (Penmetsa et al., 2003), suggesting a sensitivity to gene dosage. Intergenic noncomplementation as seen with *lss* and *sunn* can occur with alleles from the same gene when dosage is important, but it can also occur when two separate genes are acting in series or parallel in a signal cascade that is sensitive to gene dosage (Hawley and Walker, 2003). This result is consistent with the SUNN kinase signal being titrated or with SUNN acting in a multimeric complex.

Molecular and genetic tests show that *lss* is a cis-acting element that affects *SUNN* expression without affecting *SUNN* sequence: the *SUNN* gene itself is wild type but is poorly expressed from the *lss* chromosome in the *sunn LSS/SUNN lss* heterozygote (Fig. 6B). The identification of revertants in which the level of *SUNN* expression is essentially restored to wild-type levels suggests that an unstable or epigenetic mechanism may be operating to produce the phenotype. A simple explanation for the wild-type plants that appear in the F2 generation of the cross between *sunn* and *lss* may be reversion of this epigenetic effect. Analysis of *lss* RNA on the Affymetrix 50K GeneChip Medicago Genome Array Microarray showed that *SUNN* was the only

gene on the chip with altered expression in the area genetically defined to contain *LSS* (data not shown), suggesting that whatever the *lss* lesion is, its effect is specific to *SUNN*.

The lack of dramatic differences in methylation in the *SUNN* promoter region between *lss* and wild-type plants implies that promoter methylation is not a likely source of the silencing. Methylation was high near the MITE, a common occurrence in plants (Rabinowicz et al., 2003), and low to nonexistent at the transcript start site, which is common even to plant genes that undergo imprinting (Gehring et al., 2009). We also identified five bases with consistently differential methylation in *lss* compared with wild-type genomic DNA. However, the differences are small (10%–30%), and while they correlate with expression levels, the direction of the correlation is opposite to known methylation-directed control of plant gene expression. In all five cases, methylation was higher in wild-type and *lss* revertant plants that express *SUNN* than in *lss*, which expresses little *SUNN*. These latter considerations suggest to us that the small differences detected do not account for the reduction of *SUNN* expression in *lss*.

While we cannot yet rule out methylation changes elsewhere in the gene, the majority of methylation events affecting transcription in plants have been reported to occur in the promoter, within 2 kb of the gene start (Penterman et al., 2007), and methylation of exons is much rarer in plants than in mammals (Rabinowicz et al., 2003). Other possible epigenetic modifications influencing expression, such as histone modifications, will require more study. Histone methylation has been shown to play a critical role in the proper expression of some genes in plant development and is a major silencing mechanism in Arabidopsis (Vaillant and Paszkowski, 2007, Zhang et al., 2007b). It is possible that the *lss* lesion could be the loss of an insulator element, allowing histone modification to spread across *SUNN*. Alternatively, *lss* could be the loss of an enhancer element required for *SUNN* expression or a change in the histone modifications at this element. In these cases, reversion events would

occur when methylation failed to reach the required threshold for stable maintenance. However, loss of insulator or enhancer elements would have to occur outside the area already sequenced.

Knowing the identity of *lss* will be helpful to devising a model of the regulation of nodule number. If *LSS* is a DNA lesion with epigenetic effects on chromatin structure, precise localization may be difficult. The map-based cloning of *SUNN* revealed that recombination is suppressed in this area of the genome (Schnabel et al., 2003), and comparison of the genetic and physical distance in the *lss* mapping population confirms this. The recombination rate in the *lss* × A20 population is 50% lower than the suppressed level in the *sunn-1* × A20 population; our data now show that the suppressed region extends over a larger region than we originally observed when mapping *SUNN*. The *lss* lesion is in the Jemalong cultivar, while the *sunn* mutation is in the A17 genotype, which was derived from the Jemalong cultivar in *M. truncatula* and is the source genotype for genomic sequencing. It may be that genomic differences, including an unknown genome rearrangement between Jemalong and A17, might explain the suppression of recombination rate. Screening almost 3,700 progeny exhausted the mapping population without narrowing the region. For further analysis, we have undertaken a new cross to the DZA315 genotype to overcome the apparent limitations of the *lss* × A17 crosses.

In summary, our data indicate that *lss* regulates nodule number through the modification of *SUNN* expression. While *lss* mutants are similar to all *sunn* mutants on a gross morphological level, plants carrying the *lss* mutation display nodulation less sensitive to nitrate and ethylene than *sunn-1* plants, phenotypically copying the *sunn-4* presumed null allele. The reduced expression of the *SUNN* gene in the shoots of *lss* plants and in *lss* heterozygotes, and the lack of complementation of *lss* and *sunn* when heterozygous, suggest that the main effect of the *lss* lesion is to reduce *SUNN* expression. Analysis of cDNA from plants heterozygous for *sunn* and *lss* suggests that *lss* is a cis-acting factor that inhibits the expression of *SUNN*.

Table II. *Summary of molecular markers used in the mapping of lss*

Some of these markers were previously reported or are publicly available (Schnabel et al., 2003; http://www.medicago.org/genome/map.php). SNP, Single nucleotide polymorphism.

Marker Name (Type)	Primers (5′→3′)	Annealing Temperature	Enzyme	Band Size	
				A17	A20
		°C		bp	
AJ16C13B (CAPS)	CGCAGCATAGGAATCAGGTC CCAACACATTCCCCTTTTCAA	55	*Bst*UI	537	216 + 321
AJ167K21 (SNP)	AGTTGAAAGTGAGATAAGGTGAGATACATG AGTACATCCACAATCTTCCTTCC	55	–	585 T at 343	585 C at 343
ES72D11R (CAPS)	TATATTATGGTCGGAGTTCG AAATTTCTTGGTAGTAGTTAGTA	48	*Pst*I	357 + 116 + 35	357 + 151
ES10P20-2 (CAPS)	ACGGATATTCTGTCCAACCCTACCT ACTTGGGCCTTCAGTCATGCTCGTA	52	*Bst*UI	397	351 + 46

Reversion of this lack of expression occurs naturally, but lack of expression is not correlated with an increase in promoter methylation. Thus, *lss* represents either a distal novel locus within the mapped region affecting *SUNN* expression or an uncharacterized epigenetic modification at the *SUNN* locus.

MATERIALS AND METHODS

Plant Material

The seeds of all genotypes and ecotypes of *Medicago truncatula* used were scarified in concentrated sulfuric acid (American Chemical Society 93%–98%) by vortexing for 8 min in 15- or 50-mL sterile plastic tubes, depending on the quantity of seed treated. The seeds were washed in distilled water five times and rinsed once in 50% commercial bleach (6% sodium hypochlorite) followed by a final wash with distilled water five times. Treated seeds were imbibed in water shaking at 50 rpm for 3 to 4 h at room temperature. Following imbibition, the seeds were plated by suspending over sterile water, via surface tension, on the lids of sterile 15-mL petri dishes and were vernalized for at least 2 d in the dark at 4°C before being germinated in darkness at 25°C for 24 h. Germinated seedlings were grown on plates, in aeroponic chambers, or in soil as appropriate to a given experiment.

Plants used for phenotypic analysis and comparison, gene expression, and mapping purposes were grown in an aeroponic chamber on nodulation medium as described by Penmetsa and Cook (1997) with the exception of experiments testing nitrogen tolerance, in which 10 mM NH_4NO_3 or 10 mM KNO_3 was added to the medium. Plants were inoculated with wild-type *Sinorhizobium medicae* strain ABS7 (Bekki et al., 1987) 4 d after they were loaded onto the aeroponic chamber, unless otherwise indicated. This was done by adding to the chamber a solution made from a 25-mL culture that had been grown in tryptone/yeast extract medium containing 15 μg mL^{-1} tetracycline at 30°C to an optical density at 600 nm of 0.9, spun down, and resuspended in aeroponic medium.

For plate experiments, plants were grown in vertically oriented sterile Bio-Assay Dishes (245 × 245 × 25; Nunc Brand Products) with 250 mL of buffered nodulation medium (Ehrhardt et al., 1992) including 0.1 μM AVG. The plates were sealed with hypoallergenic cloth tape (Kendall), and the lower two-thirds of the plates were wrapped in aluminum foil to decrease light exposure to the roots. The plants were flood inoculated with rhizobia 4 d after they were plated, unless otherwise mentioned. For tests of plants later than 15 d after inoculations, plants were grown in a greenhouse at 20°C to 25°C with natural light supplemented with a 14-h/10-h light/dark cycle; the growth medium was Middleweight Soil Mix 3-B (Fafard), and all plants were watered daily with a 100-fold dilution of water-soluble 20:10:20 Peat-Lite Special fertilizer (Scotts).

Plant Phenotype Scoring

Plants grown on caissons or plates were scored for nodule number and root length 10 d post inoculation with rhizobia, unless otherwise noted. Root length was measured with a ruler from just below the hypocotyl junction to the root tip. Nodules were counted using a dissecting microscope.

Hormonal Treatments and Measurements

A stock solution of 100 mM ACC was prepared in 1 mL of distilled water. The stocks were filter sterilized during preparation. For ACC treatments, AVG was omitted from the growth medium.

For quantification of ethylene production, three biological replicates of aeroponically grown plants were harvested 10 d post inoculation with rhizobia. Three plants of a single genotype were pooled together into a single serum-stopper 24-mL glass vial and incubated for 4 h in the growth chamber at 25°C. Ethylene was quantified by directly injecting a 1-mL sample of the air space from the vial into a gas chromatograph (Shimadzu GC-9A) equipped with a flame photometric detector; column temperature was 30°C and injection temperature was 130°C; supply pressure was as follows: air (50 p.s.i.), H_2 (50 p.s.i.), N_2 (100 p.s.i.). Empty vials were also sampled in triplicate to account for background ethylene in the air. The fresh weight of the plants was measured, and the amount of ethylene produced was divided by the respective fresh weight.

Genetic Crosses

Artificial hybridization was performed as described by Pathipanawat et al. (1994). Emasculated buds 2 d prior to full anthesis were used for crossing purposes, as they were most amenable to cross-pollination and least prone to self-pollination (Penmetsa and Cook, 2000). Pollen was removed using a hand-held vacuum system from the pollen-recipient parent, and pollen from freshly tripped flowers of the pollen-donor parent was added to the stigma of the emasculated flowers using fine tweezers as described by Penmetsa and Cook (2000). When crossing phenotypically similar individuals, we used a male-sterile floral homeotic mutant of *M. truncatula* 'Jemalong', *Mtapetala*, to eliminate the possibility of obtaining false positives from our crosses. The *apetala* mutant did not require emasculation, and the effects of the *apetala* mutation are restricted only to floral organs; nodulation is indistinguishable from that of the wild type (Penmetsa and Cook, 2000). The resulting pods were wrapped in surgical gauze and labeled to aid collection.

Genetic Mapping

Individuals homozygous for the *lss* mutation were hand emasculated and crossed with pollen from ecotype A20, as described by Schnabel et al. (2003). The resulting F1 progeny from the *lss* × A20 cross were allowed to self-pollinate to generate multiple, independent F2 populations. Progeny from eight *lss* × A20 F1 plants were screened for the *lss* phenotype, based on the nodule number and root length. Plants assumed homozygous for the *lss* mutation based on the supernodulation phenotype were used to map the *lss* mutation by following the segregation of the mutant phenotype with CAPS markers and other molecular markers (Table II), some of which were previously developed against available EST and BAC sequences (Schnabel et al., 2003). DNA from these plants was isolated using DNeasy Plant Kits (Qiagen) and FTA Plant Cards (Whatman). The genomic DNA was used as the template to amplify PCR fragments using primer sets specific for each marker, followed by digestion with the appropriate enzyme. Gel electrophoresis and ethidium bromide staining were used to observe the genotype of the plant at that particular marker. Because each marker is inherited in a codominant fashion, all allelic combinations were readily scored. The resulting genotype assignments were observed and compiled in a color map that consisted of all plants with informative recombination events to visualize the distance between the markers that flank *lss* (Kiss et al., 1998).

Quantification of Gene Expression

Total RNA was extracted from plant tissues using the Qiagen RNeasy Plant Mini Kit according to the manufacturer's instructions. RNA was extracted from roots and shoots from 14 d-old-plants (10 d post inoculation) gathered in three independent biological replicates. Approximately 1 to 2 μg of RNA was used as the template for single-strand cDNA synthesis using random hexanucleotide primers (Invitrogen) and SuperScript Reverse Transcriptase II (Invitrogen) following the manufacturer's instructions. The same amount of RNA was used as starting material for each sample within an experiment.

In previous work (Schnabel et al., 2005), gene-specific intron-spanning primers were designed to amplify a 523-bp fragment from the kinase domain of *SUNN* cDNA. For all expression studies, the *M. truncatula SECRET AGENT* gene was used as an internal control, as described by Schnabel et al. (2005). Gene expression levels were quantified by qPCR in a Bio-Rad iCycler. Detection of gene expression levels occurred in 25-μL PCRs consisting of iQ SYBR Green Supermix (Bio-Rad). Cycling conditions were 95°C for 3 min, followed by 40 cycles of 95°C for 10 s, 61°C for 20 s, 72°C for 1 min, and 82°C for 10 s. Fluorescence data (excitation filter, 480/20; emission filter, 530/30) were collected at 82°C to prevent signal detection from primer-dimers from interfering with the signal from the specific PCR products.

PCR threshold cycles (Ct) were determined from PCR baseline-subtracted curve-fit data using default parameters of the iCycler software package. A dilution series of a known template was used for each experiment to calculate the efficiency (E) of the PCR for a given primer pair from the slope of the regression line from a plot of Ct versus log (template concentration) using the formula $E = 10^{(-1/slope)}$. For each primer pair on a biological replicate, three technical replicates were used, and average Ct values were calculated from these values.

Expression in *lss/sunn* Heterozygotes

The cDNA from F1 plants of *lss* × *sunn-2* or *lss* × *sunn-1* was analyzed with the *sunn-1* or *sunn-2* marker to determine if the heterozygote expressed either the *lss SUNN* or the *sunn-2* allele, the *sunn-1* allele, or both. cDNA from heterozygote plants, A17 wild-type plants, and genomic DNA from A17 and *sunn-2* plants were extracted as described. These were used as templates to amplify a 414-bp fragment using primers 5′-AGAATCTGAAGGTTCTAAG-CATTTT-3′ and 5′-GACACTCCACTACTTCCTCTGCT-3′ for *sunn-2* and 5′-CATGTTGCTGATTTTGGACTTG-3′ and 5′-CCTGGTACCCTAGAGATT-AATCAAGTTGTGACT-3′ for *sunn-1*. The annealing temperature used was 57°C. Following amplification, the PCR products were digested with *Bsm*AI (New England Biolabs) at 55°C for 4 h, which cuts only the *sunn-2* allele, or *Hae*III (New England Biolabs) at 37°C for 4 h, which cuts only the *sunn-1* allele. Following digestion, the samples were run on a 1% agarose gel and stained with ethidium bromide.

Bisulfite Sequencing

Genomic DNA (500 ng) from leaves of greenhouse-grown plants was converted with bisulfite using the EZ Methylation Direct Kit (Zymo Research) following the manufacturer's protocol. *SUNN* promoter fragments were amplified by PCR from bisulfite-converted DNA using primer pairs designed using Kismeth (http://katahdin.mssm.edu/kismeth/primer_design.pl) that are specific for amplification from the lower strand of converted DNA (Gruntman et al., 2008). PCR products were gel purified, extracted using UltraFree DA columns (Millipore), ethanol precipitated, and cloned using the pGEM T-Easy Vector System (Promega). Ten clones were sequenced from each region in each replicate to determine percentage methylation.

Statistical Analysis

Significance results (P values) were calculated using Student's t test in Kaleidagraph (Synergey Software).

LITERATURE CITED

Bauer WD (1981) Infection of legumes by rhizobia. Annu Rev Plant Physiol **32:** 407–449

Bekki A, Trichant JC, Rigaud J (1987) Nitrogen fixation (C₂H₂ reduction) by Medicago nodules and bacteroids under sodium chloride stress. Physiol Plant **71:** 61–67

Boot KJM, van Brussel AAN, Tak T, Spaink HP, Kijne JW (1999) Lipo-chitin oligosaccharides from *Rhizobium leguminosarum* bv. *viciae* reduce auxin transport capacity in *Vicia sativa* subsp. *nigra* roots. Mol Plant Microbe Interact **12:** 839–844

Caba JM, Recalde L, Ligero F (1998) Nitrate-induced ethylene biosynthesis and the control of nodulation in alfalfa. Plant Cell Environ **21:** 87–93

Caetano-Anollés G, Gresshoff PM (1991) Plant genetic control of nodulation. Annu Rev Microbiol **45:** 345–382

Carroll BJ, McNeil DL, Gresshoff PM (1985a) A super-nodulation and nitrate-tolerant symbiotic (nts) soybean mutant. Plant Physiol **78:** 34–40

Carroll BJ, McNeil DL, Gresshoff PM (1985b) Isolation and properties of soybean [Glycine max (L.) Merr.] mutants that nodulate in the presence of high nitrate concentrations. Proc Natl Acad Sci USA **82:** 4162–4166

Coronado C, Zuanazzi J, Sallaud C, Quirion JC, Esnault R, Husson HP, Kondorosi A, Ratet P (1995) Alfalfa root flavonoid production is nitrogen regulated. Plant Physiol **108:** 533–542

Crawford NM, Kahn ML, Leustek T, Long SR (2000) Nitrogen and sulfur. *In* BB Buchanan, W Gruissem, RL Jones, eds, Biochemistry and Molecular Biology of Plants. American Association of Plant Physiologists, Rockville, MD, pp 787–849

Ehrhardt DW, Atkinson EM, Long SR (1992) Depolarization of alfalfa root hair membrane potential by *Rhizobium meliloti* Nod factors. Science **256:** 998–1000

Gehring M, Bubb KL, Henikoff S (2009) Extensive demethylation of repetitive elements during seed development underlies gene imprinting. Science **324:** 1447–1451

Gresshoff PM, Lohar D, Chan PK, Biswas B, Jiang Q, Reid D, Ferguson BJ, Stacey G (2009) Genetic analysis of ethylene regulation of legume nodulation. Plant Signal Behav **4:** 818–823

Gruntman E, Qi Y, Slotkin RK, Roeder T, Martienssen RA, Sachidanandam R (2008) Kismeth: analyzer of plant methylation states through bisulfite sequencing. BMC Bioinformatics **9:** 371

Hawley RS, Walker MY (2003) Advanced Genetic Analysis: Finding Meaning in a Genome. Blackwell Publishing, Malden, MA

Higo K, Ugawa Y, Iwamoto M, Korenaga T (1999) Plant cis-acting regulatory DNA elements (PLACE) database: 1999. Nucleic Acids Res **27:** 297–300

Hirsch AM, Fang Y (1994) Plant hormones and nodulation: what's the connection? Plant Mol Biol **26:** 5–9

Huo X, Schnabel E, Hughes K, Frugoli J (2006) RNAi phenotypes and the localization of a protein:GUS fusion imply a role for *Medicago truncatula PIN* genes in nodulation. J Plant Growth Regul **25:** 156–165

Ishikawa K, Yokota K, Li YY, Wang Y, Liu C, Suzuki S, Aono T, Oyaizu H (2008) Isolation of a novel root-determined hypernodulation mutant *rdh1* of *Lotus japonicus*. Soil Sci Plant Nutr **54:** 259–263

Jacobsen E, Feenstra WJ (1984) A new pea mutant with efficient nodulation in the presence of nitrate. Plant Sci Lett **33:** 337–344

Kiss GB, Kereszt A, Kiss P, Endre G (1998) Colormapping: a non-mathematical procedure for genetic mapping. Acta Biol Hung **49:** 125–142

Kosslak RM, Bohlool BB (1984) Suppression of nodule development of one side of a split-root system of soybeans caused by prior inoculation of the other side. Plant Physiol **75:** 125–130

Krusell L, Madsen LH, Sato S, Aubert G, Genua A, Szczyglowski K, Duc G, Kaneko T, Tabata S, de Bruijn FJ, et al (2002) Shoot control of root development and nodulation is mediated by a receptor-like kinase. Nature **420:** 422–426

Kuppusamy KT, Endre G, Prabhu R, Penmetsa RV, Veereshlingam H, Cook DR, Dickstein R, VandenBosch KA (2004) *LIN*, a *Medicago truncatula* gene required for nodule differentiation and persistence of rhizobial infections. Plant Physiol **136:** 3682–3691

Magori S, Oka-Kira E, Shibata S, Umehara Y, Kouchi H, Hase Y, Tanaka A, Sato S, Tabata S, Kawaguchi M (2009) *Too much love*, a root regulator associated with the long-distance control of nodulation in *Lotus japonicus*. Mol Plant Microbe Interact **22:** 259–268

Mathesius U, Charon C, Rolfe BG, Kondorosi A, Crespi M (2000) Temporal and spatial order of events during the induction of cortical cell divisions in white clover by Rhizobium leguminosarum bv. trifolii inoculation or localized cytokinin addition. Mol Plant Microbe Interact **13:** 617–628

Mathesius U, Schlaman HR, Spaink HP, Of Sautter C, Rolfe BG, Djordjevic MA (1998) Auxin transport inhibition precedes root nodule formation in white clover roots and is regulated by flavonoids and derivatives of chitin oligosaccharides. Plant J **14:** 23–34

Nishimura R, Hayashi M, Wu GJ, Kouchi H, Imaizumi-Anraku H, Murakami Y, Kawasaki S, Akao S, Ohmori M, Nagasawa M, et al (2002a) HAR1 mediates systemic regulation of symbiotic organ development. Nature **420:** 426–429

Nishimura R, Ohmori M, Fujita H, Kawaguchi M (2002b) A Lotus basic leucine zipper protein with a RING-finger motif negatively regulates the developmental program of nodulation. Proc Natl Acad Sci USA **99:** 15206–15210

Oka-Kira E, Kawaguchi M (2006) Long-distance signaling to control root nodule number. Curr Opin Plant Biol **9:** 496–502

Oka-Kira E, Tateno K, Miura K, Haga T, Hayashi M, Harada K, Sato S, Tabata S, Shikazono N, Tanaka A, et al (2005) *klavier* (*klv*), a novel hypernodulation mutant of *Lotus japonicus* affected in vascular tissue organization and floral induction. Plant J **44:** 505–515

Oldroyd GE, Downie JA (2008) Coordinating nodule morphogenesis with rhizobial infection in legumes. Annu Rev Plant Biol **59:** 519–546

Oldroyd GED, Engstrom EM, Long SR (2001) Ethylene inhibits the Nod factor signal transduction pathway of *Medicago truncatula*. Plant Cell **13:** 1835–1849

Pacios-Bras C, Schlaman HRM, Boot KJM, Admiraal P, Langerak JM,

Stougaard J, Spaink HP (2003) Auxin distribution in *Lotus japonicus* during root nodule development. Plant Mol Biol **52:** 1169–1180

Park SJ, Buttery BR (1989) Inheritance of nitrate-tolerant supernodulation in EMS-induced mutants of common bean (*Phaseolus vulgaris* L.). J Hered **80:** 486–488

Pathipanawat W, Jones RAC, Sivasithamparam K (1994) An improved method for artificial hybridization in annual Medicago species. Aust J Agric Res **45:** 1329–1335

Penmetsa RV, Cook DR (1997) A legume ethylene-insensitive mutant hyperinfected by its rhizobial symbiont. Science **275:** 527–530

Penmetsa RV, Cook DR (2000) Production and characterization of diverse developmental mutants of *Medicago truncatula*. Plant Physiol **123:** 1387–1398

Penmetsa RV, Frugoli J, Smith L, Long SR, Cook D (2003) Genetic evidence for dual pathway control of nodule number in *Medicago truncatula*. Plant Physiol **131:** 998–1008

Penmetsa RV, Uribe P, Anderson J, Lichtenzveig J, Gish JC, Nam YW, Engstrom E, Xu K, Sckisel G, Pereira M, et al (2008) The Medicago truncatula ortholog of Arabidopsis EIN2, sickle, is a negative regulator of symbiotic and pathogenic microbial associations. Plant J **55:** 580–595

Penterman J, Zilberman D, Huh JH, Ballinger T, Henikoff S, Fischer RL (2007) DNA demethylation in the Arabidopsis genome. Proc Natl Acad Sci USA **104:** 6752–6757

Prayitno J, Rolfe BG, Mathesius U (2006) The ethylene-insensitive *sickle* mutant of *Medicago truncatula* shows altered auxin transport regulation during nodulation. Plant Physiol **142:** 168–180

Rabinowicz PD, Palmer LE, May BP, Hemann MT, Lowe SW, McCombie WR, Martienssen RA (2003) Genes and transposons are differentially methylated in plants, but not in mammals. Genome Res **13:** 2658–2664

Riely BK, Mun JH, Ané JM (2006) Unravelling the molecular basis for symbiotic signal transduction in legumes. Mol Plant Pathol **7:** 197–207

Sagan M, Duc G (1996) *Sym28* and *Sym29*, two new genes involved in regulation of nodulation in pea (*Pisum sativum* L). Symbiosis **20:** 229–245

Schnabel E, Journet EP, de Carvalho-Niebel F, Duc G, Frugoli J (2005) The Medicago truncatula SUNN gene encodes a CLV1-like leucine-rich repeat receptor kinase that regulates nodule number and root length. Plant Mol Biol **58:** 809–822

Schnabel E, Kulikova O, Penmetsa RV, Bisseling T, Cook DR, Frugoli J (2003) An integrated physical, genetic and cytogenetic map around the sunn locus of Medicago truncatula. Genome **46:** 665–672

Searle IR, Men AE, Laniya TS, Buzas DM, Iturbe-Ormaetxe I, Carroll BJ, Gresshoff PM (2003) Long-distance signaling in nodulation directed by a CLAVATA1-like receptor kinase. Science **299:** 109–112

Stacey G, Libault M, Brechenmacher L, Wan J, May GD (2006) Genetics and functional genomics of legume nodulation. Curr Opin Plant Biol **9:** 110–121

Subramanian S, Stacey G, Yu O (2006) Endogenous isoflavones are essential for the establishment of symbiosis between soybean and Bradyrhizobium japonicum. Plant J **48:** 261–273

Subramanian S, Stacey G, Yu O (2007) Distinct, crucial roles of flavonoids during legume nodulation. Trends Plant Sci **12:** 282–285

Vaillant I, Paszkowski J (2007) Role of histone and DNA methylation in gene regulation. Curr Opin Plant Biol **10:** 528–533

van Noorden GE, Ross JJ, Reid JB, Rolfe BG, Mathesius U (2006) Defective long-distance auxin transport regulation in the *Medicago truncatula super numeric nodules* mutant. Plant Physiol **140:** 1494–1506

Wopereis J, Pajuelo E, Dazzo FB, Jiang Q, Gresshoff PM, De Bruijn FJ, Stougaard J, Szczyglowski K (2000) Short root mutant of *Lotus japonicus* with a dramatically altered symbiotic phenotype. Plant J **23:** 97–114

Zhang J, Subramanian S, Zhang Y, Yu O (2007a) Flavone synthases from *Medicago truncatula* are flavanone-2-hydroxylases and are important for nodulation. Plant Physiol **144:** 741–751

Zhang X, Clarenz O, Cokus S, Bernatavichute YV, Pellegrini M, Goodrich J, Jacobsen SE (2007b) Whole-genome analysis of histone H3 lysine 27 trimethylation in Arabidopsis. PLoS Biol **5:** e129